Available online at www.sciencedirect.com
ScienceDirect
ELSEVIER
Palaeogeography, Palaeoclimatology, Palaeoecology 247 (2007) 313–328
PALAEO
www.elsevier.com/locate/palaeo

Climatic variation in the Linxia basin, NE Tibetan Plateau, from 13.1 to 4.3 Ma: The stable isotope record

Majie Fan [a,b,*], David L. Dettman [a], Chunhui Song [b], Xiaomin Fang [b,c], Carmala N. Garzione [d]

[a] Department of Geosciences, University of Arizona, Tucson, Arizona 85721, USA
[b] Key Laboratory of Western China's Environmental Systems (Ministry of Education) and College of Earth and Environment Sciences, Lanzhou University, Lanzhou, Gansu 730000, PR China
[c] Institute of Tibetan Plateau Research, Chinese Academy of Science, Beijing 100085, PR China
[d] Department of Earth and Environmental Sciences, University of Rochester, Rochester, NY 14627, USA

Received 23 December 2005; received in revised form 27 October 2006; accepted 3 November 2006

Abstract

The $\delta^{13}C$ and $\delta^{18}O$ values of carbonates and $\delta^{13}C_{org}$ values, % C, and C/N ratios of organic matter from lacustrine and fluvial sediments were measured from two stratigraphic sections in the Linxia basin on the northeastern margin of the Tibetan Plateau. Diagenesis, when present, is early, limited to small spatial scales and restricted stratigraphic intervals. A strong correlation exists between dolomite content and the $\delta^{18}O$ values of micritic carbonate suggesting that carbonates are primary precipitates from lake water and that $\delta^{18}O$ values reflect changes in the lake environment, with more positive values derived from evaporated and more saline lake water. The first part of this record is characterized by strong oscillations between dry and wet conditions accompanied by changes in the lake system between hydrographically closed and open states (13.1–8.0 Ma). The most severe aridity occurred from 9.6 to 8.5 Ma. After ~8.0 Ma, a more stable and less arid climate dominated the region and the drainage system was open (8.0–5.3 Ma). After 5.3 Ma, climate became gradually drier and/or cooler (5.3–4.3 Ma).

The organic matter preserved in the Linxia basin is most likely a mixture of terrestrial C_3 plant matter and lake algae. A correlation between C/N and $\delta^{13}C_{org}$ indicates that a significant percentage of the organic matter is derived from terrestrial sources. The organic matter has undergone selective degradation during which the C/N ratios and organic carbon percentage decreased. The $\delta^{13}C_{org}$ values are relatively stable throughout the 13.1 to 4.3 Ma interval ranging from −24 to −29‰ VPDB, suggesting that C_4 grasses were either absent or insignificant in the Linxia region prior to 4.3 Ma.

Keywords: Linxia basin; Oxygen isotope; Organic matter; Diagenesis; Tibetan Plateau

1. Introduction

Long-term climate records from marine environments reveal important trends in global climate throughout the Cenozoic: cooling since the late Cretaceous, warming in the Eocene and then a progressive step-wise cooling, more pronounced since the mid-Miocene, culminating in the glacial/interglacial cycles of the Pleistocene (e.g., Rea et al., 1998; Lear et al., 2000; Zachos et al., 2001; Billups and Schrag, 2002; Zheng et al., 2004). The $\delta^{18}O$ and Mg/Ca records of benthic foraminifers show a general cooling trend since

* Corresponding author. Department of Geosciences, University of Arizona, Tucson, Arizona 85721, USA. Fax: +1 520 621 2672.
E-mail address: mfan@email.arizona.edu (M. Fan).

0031-0182/$ - see front matter © 2006 Elsevier B.V. All rights reserved.
doi:10.1016/j.palaeo.2006.11.001

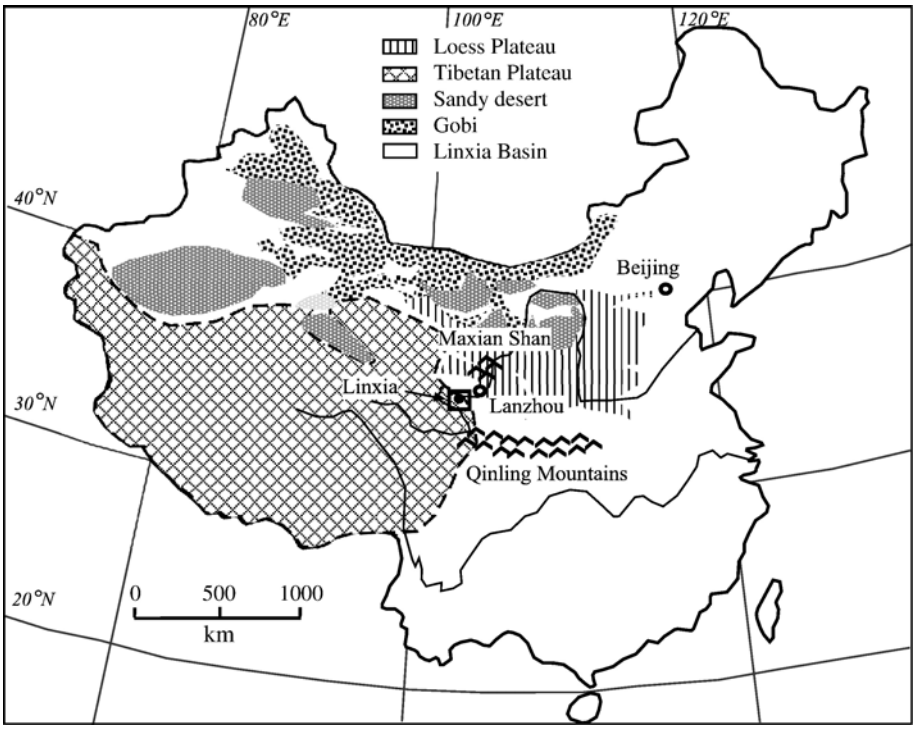

Fig. 1. Location of the study area relative to major geographical features in China.

the mid-Miocene, thought to be driven by the growth of the East Antarctic ice sheet and subsequent cooling of Antarctic Bottom Water (Lear et al., 2000; Zachos et al., 2001; Billups and Schrag, 2002).

In East Asia, climate change since the mid-Miocene is particularly interesting since it is a critical period in the history of uplift of the Tibetan Plateau. Currently most of the climate records in this region are from eolian Red Clay and loess sequences, which have yielded high-resolution climate records spanning the last ~8 Ma (An et al., 2001; Ding et al., 2001). Climate records prior to 8 Ma are rare in this region, due to the apparent lack of older continuous loess deposits (see, however, Fan et al., 2006) while the eolian record mostly reflects climate change in the loess source region, i.e. the sandy deserts of northwestern China (Sun, 2002). Lake systems are excellent potential archives of climatically responsive sediments where geochemical tracers can be used to reconstruct long-term (million-year) climate records. The stable isotope geochemistry of organic matter and authigenic carbonate in lake sediments can be a sensitive proxy of environmental and hydrological changes driven by climate variation (Meyers and Benson, 1988; Last, 1990; Talbot, 1990; Dean and Stuiver, 1993; Meyers and Ishiwatari, 1993; Drummond et al., 1995; Li and Ku, 1997; Meyers, 1994, 1997; Kashiwaya et al., 2001; Meyers, 2003). The northeastern edge of the Tibetan Plateau holds good potential for this kind of study, as it is an area where foreland basins have collected sediment over much of the Cenozoic (Métivier et al., 1998; Fang et al., 2003; Horton et al., 2004). The lake deposits filling these basins preserve both organic matter from the lake environment and terrestrial plant matter within the lake drainage system. In addition, they contain authigenic carbonate precipitated from lake water. If major diagenetic alteration can be ruled out for the lake sediments, we should be able to use these techniques to provide a record of environmental and climatic change at the northwestern edge of the Tibetan Plateau.

In this paper, we studied two outcrop sections in the Linxia basin on the northeastern edge of the Tibetan Plateau, focusing on the stable isotope geochemistry of sediments in the basin. Dettman et al. (2003) reported a lower resolution carbonate isotope record of the Maogou section covering the last 29 Ma in the Linxia basin. They concluded that there was a significant shift in the $\delta^{18}O$ of meteoric water in the basin sometime between 13 and 12 Ma, which was most likely the result of uplift of some portion of the Tibetan Plateau to an elevation that blocked Pacific or Indian Ocean moisture from reaching the region north-east of the plateau. Our study focuses on the post 13.1 Ma record and significantly

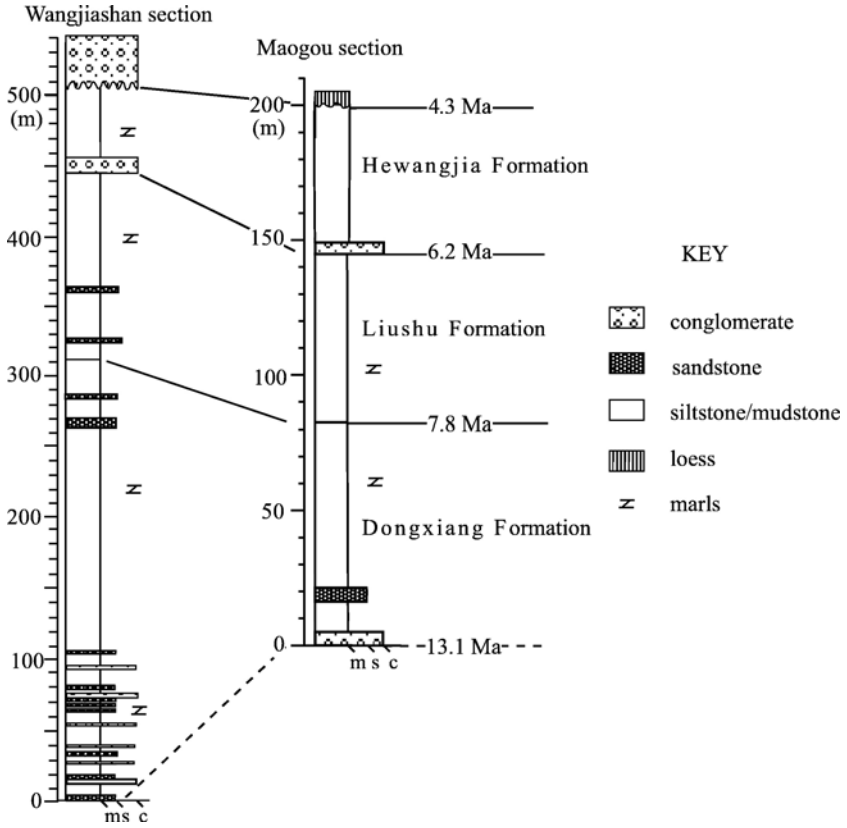

Fig. 2. Stratigraphic correlation between two measured sections in the Linxia basin. Solid lines are based on magnetostratigraphic correlation. Dashed lines are correlations based on lithofacies and mammalian fauna. See Fang et al. (2003) and Fan et al. (2006) for a geologic map of the basin and discussion of the sedimentology of these sections.

increases the sample density over that of Dettman et al. (2003). Our results provide a long-term climate and environmental history for northwestern China from the middle Miocene into the early Pliocene (13.1 to 4.3 Ma). The similarity of this record to some major features in the marine stable isotope record derived from benthic foraminifera suggests that the reconstruction is not merely a local record, but reflects broad regional and/or global climate change.

2. Regional setting, climate and stratigraphy

Located 100 km southwest of the city of Lanzhou, the Linxia basin is at the northeastern edge of the Tibetan Plateau and on the western margin of the Loess Plateau. To the north lie the deserts of west/central China and Inner Mongolia (Fig. 1). The basin is ~200 km long and 75 km wide at a current elevation of 2–2.6 km. The oldest documented sedimentary rocks in the basin are ~29 Ma old and the sedimentary package is more than 1 km thick. The basin fill thins and pinches out at the Maxian Shan to the northeast (Fang et al., 1995, 2003). Southwest of the Linxia basin, the northeastern margin of the Tibetan Plateau is delineated by the western Qinling mountains, which are made up of Devonian through Permian metasedimentary terrestrial and marine deposits and plutons of Early Paleozoic and Late Paleozoic–Early Mesozoic age (Garzione et al., 2005 and references therein). On the northern edge of Linxia basin, the Maxian Shan is underlain by Jurassic to Paleocene terrestrial deposits (Gansu Geologic Bureau, 1989). The basin is elongate parallel to the fold thrust belt on the northeastern edge of the Tibetan Plateau. Subsidence history and stratigraphic studies of three measured sections show that the Linxia basin was formed under flexural loading during the thickening of the northeastern margin of the Tibetan Plateau between ~29 and 6 Ma. Between ~8 and 6 Ma the basin was incorporated into the deformation front of the Tibetan Plateau (Fang et al., 2003).

The modern climate in northwest China is semi-arid continental with the annual average temperature in the city of Linxia (near the center of the basin) of 6.7 °C,

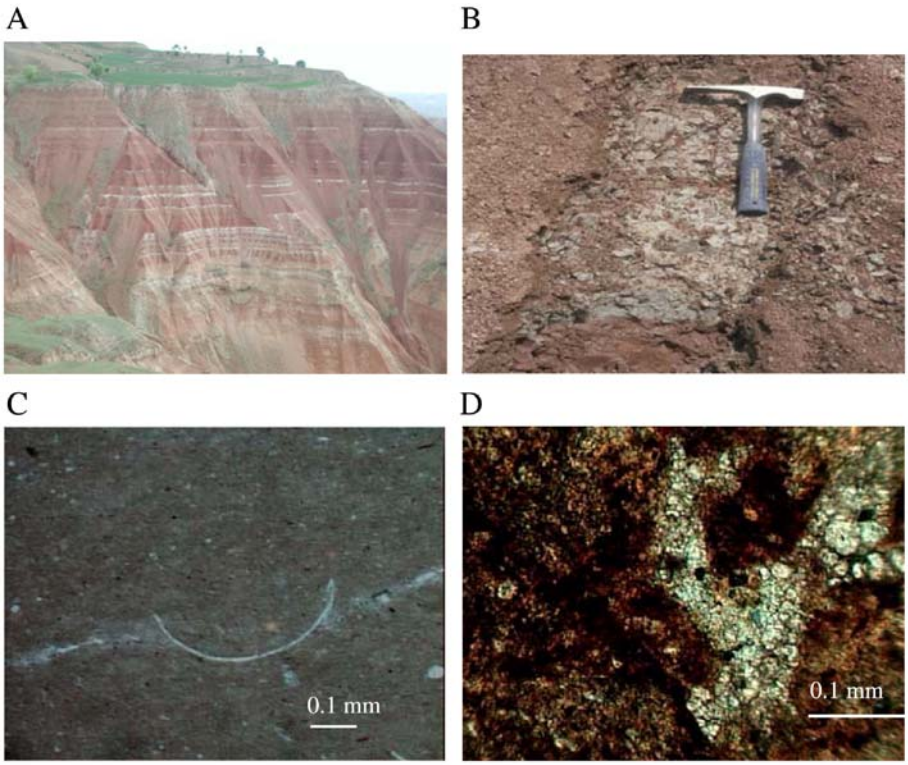

Fig. 3. Linxia basin sediments (A) Lacustrine deposits between 13 and 6 Ma. Light beds are marls and micritic limestones. (B) Sharp contact between marl and underlying siliciclastic lacustrine sediments. (C) Ostracode shell in the Dongxiang Formation. (D) Discrete zones of micrite recrystallization observed in thin section.

and an average monthly maximum temperature (in July) of 18 °C. The average annual precipitation is 500 mm with more than 85% from summer monsoon precipitation (http://www.weatherbase.com). The East Asian summer monsoon brings warm moist air from the Pacific, while the cold and dry Asian winter monsoon dominates in winter.

Our stable isotope records come from two sections, at Wangjiashan (WJS) and at Maogou. WJS is along the southwest edge of the basin, near the northeastern margin of the Tibetan Plateau, whereas the Maogou section is near the geographical center of the basin (Fig. 2). The Maogou section and the upper 500 m of WJS are well dated based on strata contain fossil mammals and two

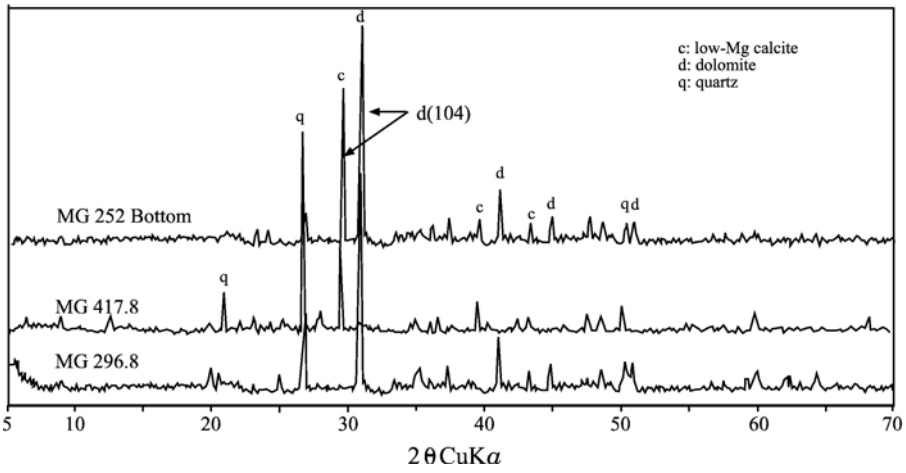

Fig. 4. XRD traces of representative samples in the Linxia basin. Note shift in position of d(104) peak corresponding to LMC and dolomite.

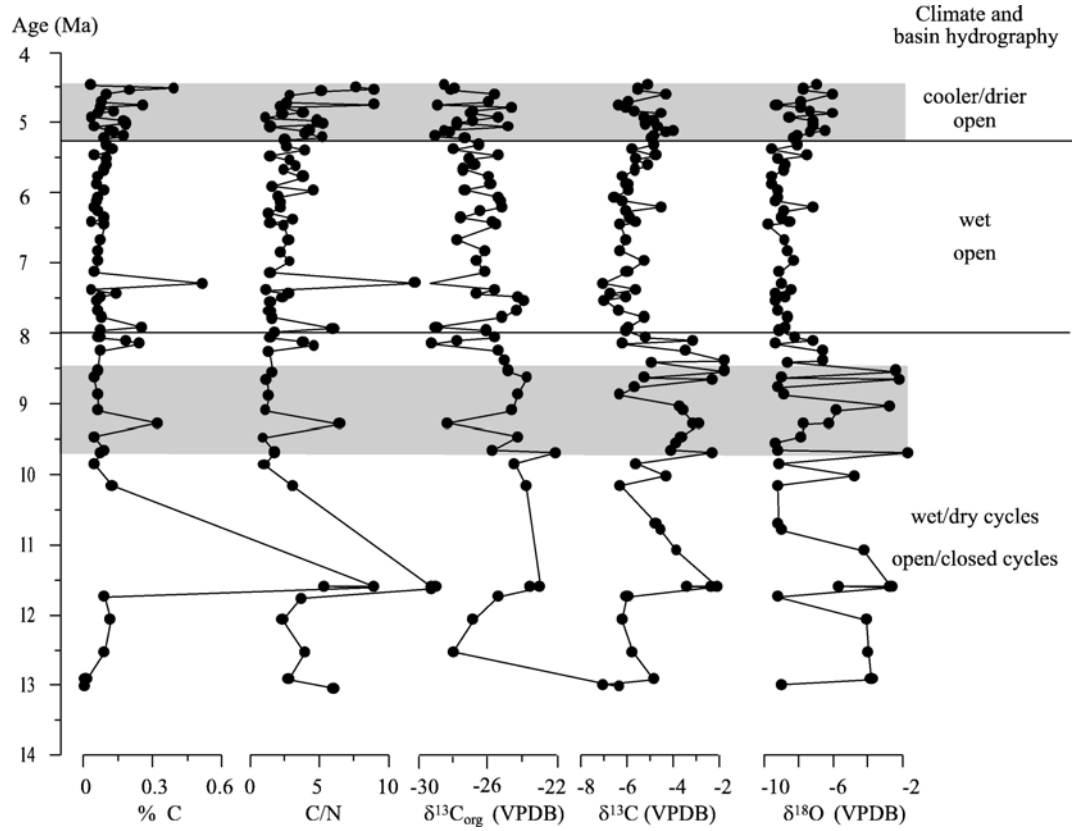

Fig. 5. Organic carbon content, C/N, $\delta^{13}C_{org}$ of bulk organic matter, $\delta^{13}C$ and $\delta^{18}O$ of carbonates in the Maogou section. Shaded areas indicate the highest $\delta^{18}O$ in 9.6–8.5 Ma and the increase after 5.3 Ma. Solid lines separate three different climate intervals in the record.

paleomagnetic polarity studies (Fang et al., 1995, 2003). The most recent magnetostratigraphy study sampled the Maogou section at 0.5–1 m intervals and WJS at 2 m intervals (Fang et al., 2003). The stratigraphy in the Linxia basin during the 13.1 and 4.4 Ma interval covered by this study is divided into three formations based on lithofacies and paleontological evidence: the Dongxiang Formation (13.1–7.8 Ma), the Liushu Formation (7.8–6.2 Ma), and the Hewangjia Formation (6.2–4.3 Ma) (Fang et al., 1995, 2003). Sedimentary facies analysis shows that the depositional environment at the measured section localities evolved from deltaic (13.1–11.0 Ma) to lacustrine (11.0–6.2 Ma) (Fan et al., 2006). The lacustrine sediments are characterized by many discrete white to gray marls with thicknesses ranging from 2 to 20 cm. These carbonates have been interpreted as primary precipitates from lake water which was supersaturated with respect to carbonate (Dettman et al., 2003; Garzione et al., 2004). A detailed grain-size study of the Maogou section shows that after 6.0 Ma, eolian sediments dominate the floodplain deposition at the Maogou section, while lacustrine deposition continues irregularly in the WJS (Fan et al., 2006) (Fig. 2).

3. Sampling and experimental methods

Carbonate-rich mudstone/siltstone, dolomitic marls, calcitic marls and mixed marls were taken from fresh outcrops of the upper WJS and the Maogou section (Fig. 2). The ages assigned to sediments were derived from the linear interpolation between geomagnetic polarity reversals (Fang et al., 1995, 2003). Reworked Permian/Triassic-age limestone clasts from fluvial channel deposits and modern soil carbonate (forming under granite cobbles in a soil zone) at 3.4 km elevation on the northeastern edge of the Tibetan Plateau were also collected for carbonate isotope analysis. Sampling occurred at two different time scales. First, we focused on a high-resolution study of millimeter-to-centimeter scale isotope variation within the typical carbonate-dominated layers. We sampled shell fragments, void fillings, carbonate inter-clast cement and reworked limestone clasts in gravels, detrital carbonate clasts, detrital clay-rich clasts and secondary veins in siltstone, mudstone, and micritic marls. For this work, only carbonate oxygen and carbon isotope values were analyzed. A second sample set was collected for a

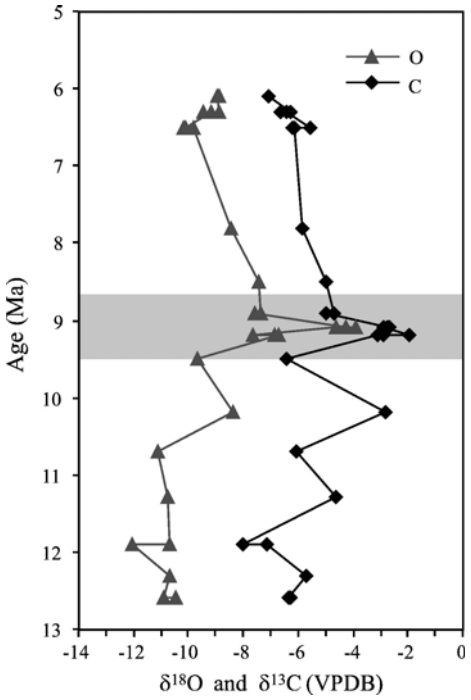

Fig. 6. Oxygen and carbon isotope composition of carbonates in the Wangjiashan section (WJS). Note the most enriched $\delta^{18}O$ values around 9 Ma, consistent with the most positive $\delta^{18}O$ values at that time in the Maogou section.

relatively low-resolution study of isotopic trends through time. The resolution of this sample set is controlled by the presence of carbonate sediments in the measured section. Data collected for the low-resolution study include, carbonate isotope ratios, organic carbon isotopes ($\delta^{13}C_{org}$), organic carbon content (% C) and C_{org}/N_{total} ratios (C/N) of the bulk organic matter. Organic matter data were not produced for the WJS section.

Polished thin sections were prepared from two fairly typical, weakly lithified, micritic marls (MG252 and MG362) cut perpendicular to the horizontal plane of sedimentary bedding. The two samples were examined petrographically and high-resolution samples were taken across the vertical cross-section. Selected samples were also powdered for X-ray diffraction, which was performed with a Bruker D8 Advance Diffractometer using Cu Kα radiation, and the carbonate mineralogy was determined based on the position of the d(104) peak. MG 362 is calcitic, whereas MG 252 is a mix of dolomite and low magnesium calcite.

The $\delta^{13}C$ and $\delta^{18}O$ values of carbonates were measured using the method described in Dettman et al. (2003). The precision of repeated standards is ± 0.12‰ for $\delta^{18}O$ and ±0.09‰ for $\delta^{13}C$ (1σ). For the analysis of $\delta^{13}C_{org}$ values, % C, % N and C/N ratios, samples were reacted with 10 ml of 10% HCl overnight to remove the carbonate and then washed by distilled water to neutral pH. Carbonate-rich samples were treated twice. The % C, % N and C/N ratios were measured by placing oven-dried samples in tin capsules combusted at 1030 °C in a Costech Elemental Analyzer. Detection limits for the elemental analyzer are 10 μg C and 20 μg N. Uncertainty based on replicates of standard materials at the minimum sample size used for unknowns was 2.7% of total nitrogen content and 1.5% of total carbon content (1σ). The $\delta^{13}C_{org}$ values were measured using a Finnigan Delta Plus XL mass spectrometer that is connected via a Finnigan MAT Conflo III split interface. $\delta^{13}C_{org}$ values were calibrated using USGS-24 and NBS-22, for which the precision is better than ±0.1‰ (1σ). All carbon isotope results are reported relative to VPDB.

4. Results

4.1. Field observation, petrology and mineralogy

Marls in the Dongxiang and Liushu Formations display a sharp contact with the surrounding lacustrine siliciclastic sediments (Fig. 3A,B). They are all clay rich and most contain siliciclastic silts. Most of the marls are massive, and only a few laminated marls were found in the Maogou section. Poorly preserved shell fragments were observed with a hand lens in some of the massive marls in the Dongxiang and Liushu Formations. Thin section study shows that the shell fragments are ostracodes — shell cross-sections with vestibule are clearly visible (Fig. 3C). Marls are micritic, with small regions of micrite recrystallization or void filling cements observed in thin

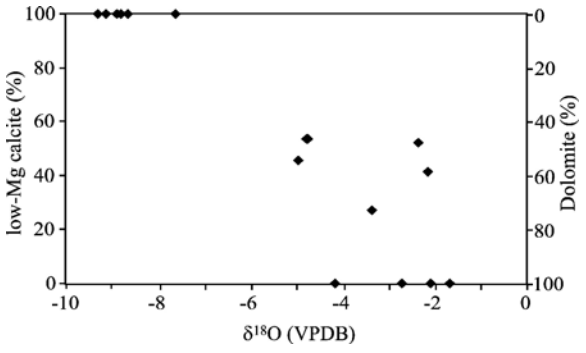

Fig. 7. Correlation of carbonate mineralogy and $\delta^{18}O$ values. This suggests that the $\delta^{18}O$ values of lacustrine carbonates reflect the degree of closure of the lake system-dolomite with high $\delta^{18}O$ values formed from saline evaporated lake water when the lake is closed. Samples are from both the Maogou section and WJS.

sections (Fig. 3D). X-ray diffraction shows that low-Mg calcite (LMC) is the dominant carbonate mineral in the marls although some intervals are dominated by dolomite. Mixtures of low-Mg calcite and dolomite are also present (Fig. 4). In fluvial sediments carbonates are primarily matrix cements associated with both eolian silts and occasional sands and gravels. These cements (in the Hewangjia Formation) are low-Mg calcite.

4.2. Carbonate stable isotopes

The carbonate isotope record shown for the Maogou section (Fig. 5) is a composite based on samples from the deltaic, lacustrine and fluvial facies. The $\delta^{18}O$ values in 13.1–8.0 Ma period are characterized by high frequency oscillations between a relatively stable end member around −9.3‰ and a more variable and more positive end member ranging up to −1.7‰. The most positive values occur between 9.6 to 8.5 Ma. After 8.0 Ma $\delta^{18}O$ values are more uniform at around −8.8‰ up to 5.3 Ma. After 5.3 Ma, the $\delta^{18}O$ values of LMC carbonates cementing fluvial sediments increase, averaging about −7.5‰. Between 13.1 and 8.0 Ma there is a strong covariance between $\delta^{13}C$ values and $\delta^{18}O$ values in the lacustrine carbonates, with $\delta^{13}C$ ranging between −7.0‰ and −2.3‰. After 7.8 Ma, $\delta^{13}C$ values stabilize at around −5.8‰. They increase slightly to −5‰ after 5.3 Ma. In the WJS section $\delta^{18}O$ and $\delta^{13}C$ values range between −12.8‰ to −5.3‰ and −7.9‰ to −2.7‰, respectively (Fig. 6). Because sampling density in the WJS section is much lower than in the Maogou section, we cannot make a detailed isotopic comparison. However, the record does show very positive values around 9 Ma, which probably corresponds to the most positive $\delta^{18}O$ values in the Maogou section at 9.6–8.5 Ma.

There is a strong relationship between the $\delta^{18}O$ values of the carbonate and its mineralogy, with more negative $\delta^{18}O$ values associated with LMC, the most positive $\delta^{18}O$ values associated with dolomite, and mixtures associated with intermediate $\delta^{18}O$ values (Fig. 7). We have not performed XRD on all marl samples, but we suspect that this relationship holds for the lacustrine record. The $\delta^{18}O$ values of subsamples from laminated marl sample MG252 and massive marl MG362 reveal two different patterns (Fig. 8). In the laminated marl, $\delta^{18}O$ values vary significantly in different layers, which also follow the mineralogical changes described above (i.e. samples containing dolomite have more positive $\delta^{18}O$ values). In the massive sample there is little variation in oxygen isotope ratios.

4.3. $\delta^{13}C_{org}$, % C and C/N ratios of bulk organic matter

The range in organic matter $\delta^{13}C_{org}$ values is relatively limited, between −29‰ and −24‰. With a few exceptions C/N ratios are between 1 and 4 throughout the section although there is a trend toward higher values after 5.3 Ma (Fig. 5). *% C* is mostly less than 0.3 %. Inorganic nitrogen was not removed from the sediment samples before combustion for measurement of the C/N ratio. Because the content of both organic carbon and nitrogen was extremely low in the study section (typically *% N* is less than 0.2 %), inorganic nitrogen may play a significant role in measured C/N ratio (Meyers, 1997, 2003).

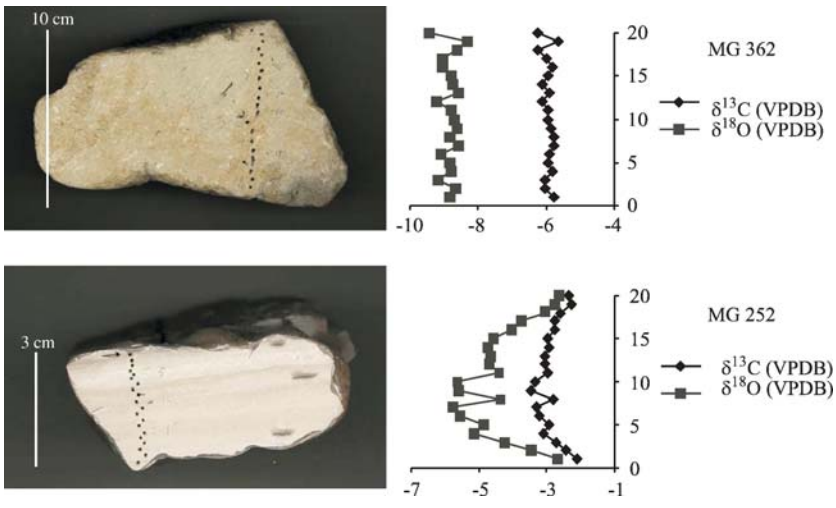

Fig. 8. Oxygen and carbon isotope composition across two weakly lithified micritic marls in the Linxia basin, laminated MG 252 and massive MG 362 (from 252 m and 362 m in the Maogou section).

5. Discussion

5.1. Carbonate diagenesis

Stable isotope ratios of unaltered carbonates preserved in lacustrine and fluvial sediments have been used to reconstruct regional temperature, paleoelevation, meteoric water source or evaporation/precipitation (Last, 1990; Talbot, 1990; Drummond et al., 1995; Li and Ku, 1997; Garzione et al., 2004). But before using this approach, one must evaluate diagenesis of the carbonates under study and its possible impact on the original stable isotope geochemistry. There is some evidence for carbonate diagenesis in the Linxia basin. (1), Areas of micrite recrystallization clearly indicate that there is some alteration of carbonate present (Fig. 3D). (2), At some stratigraphic levels, carbonates of different morphologies (vein cements, coating cements, micrite, or shell) may have very similar stable isotope values, which could be the result of diagenesis which may cause a homogenization of stable isotope ratios (e.g. MG362 in Fig. 8, or CHOO10 and MG329 in Table 1). (3), Dolomitic marls are present in the Linxia basin lacustrine sediments. Dolomite is often the product of the stabilization of formerly metastable carbonates. Original high-magnesium calcites or "protodolomite" can be replaced by more stable phases, and dolomitization can also occur through the reaction of limestone with basinal brines during deep burial (Warren, 2000).

We also note that if diagenesis occurred under modern surface conditions, the resulting $\delta^{18}O$ value of the diagenetic carbonate would have a very similar value to the −9 to −10‰ value that dominates the Miocene/Pliocene record. Modern soil carbonates at an elevation of 3.4 km on the northeastern edge of the Tibetan Plateau yielded $\delta^{18}O$ values ranging from −9.4 to −11.2‰ (Table 1, Fig. 9). The $\delta^{18}O$ value of the modern summer surface waters in the Linxia basin ranges from −8.5 to −10.4‰ (VSMOW) (Garzione et al., 2004). The calculated $\delta^{18}O$ value of the soil carbonate (calcite) precipitated from modern rainfall is −7.0 to −11.3‰ using the standard calcite oxygen isotope fractionation and a temperature between 7 and 18 °C (Kim and O'Neil, 1997). This overlaps with the modern carbonate data suggesting that this soil carbonate, forming on the underside of cobbles, was precipitated from modern rainfall under equilibrium conditions.

Note, however, that this possible diagenesis is clearly limited to small stratigraphic intervals. Morphologically, micrite recrystallization is limited to very small areas, shell fragments are preserved with very sharp edges, and the contacts between carbonate layers and siliciclastic sediments tend to be sharp, suggesting the diagenesis has not greatly redistributed carbonate in Linxia. Also we see significant and rapid change in $\delta^{18}O$ values across the two measured sections and within the 3 cm thick section of MG 252 (Figs. 5,6,8). The multiple large shifts in $\delta^{18}O$ and $\delta^{13}C$ values on both the centimeter and meter scale would not be expected to survive regional diagenetic alteration. In addition, dolomites are not always diagenetic in lacustrine systems. Quaternary dolomites with high $\delta^{18}O$ values are sometimes found in saline lakes or in sediments interpreted as deposited in a closed, saline phase of a lacustrine sedimentary package (Last, 1990). In the Linxia basin, high $\delta^{18}O$ and $\delta^{13}C$ values of dolomite-rich lake sediments indicate that lake conditions were very different than that of times when low-magnesium calcites precipitate. The strong correlation of low $\delta^{18}O$ values with low Mg-calcite and high $\delta^{18}O$ values with dolomitic micrite would be expected if this lake system was undergoing periodic closure and evaporative enrichment of the lake water (Fig. 7). Evaporation would lead to much more positive $\delta^{18}O$ values and increased salinity in the lake system, which could lead to dolomite or proto-dolomite formation in waters with elevated $\delta^{18}O$ values. Although the fractionation between water and dolomite is poorly known at low temperatures, recent work suggests that simple mineralogical differences would explain only 2 to 3‰ of the difference between calcite and dolomite in the lacustrine environment (Vasconcelos et al., 2005; Schmidt et al., 2005). The fact that the differences are up to 8‰ suggests that lake water evaporation is also involved (Fig. 7). If dolomite resulted from late, higher temperature, diagenetic alteration of original calcite, we would expect much more negative $\delta^{18}O$ values, incipient lithification of the sediments, and a more pervasive alteration of all the carbonate beds, not alternating dolomite and low Mg-calcite beds.

Therefore the diagenesis observed in the Linxia basin is most likely very early, occurring either shortly after each carbonate layer was deposited or on a very small spatial scale. Early diagenesis, in the presence of lake water or shallow groundwater and at surface temperatures would result in very little modification of the original carbonate oxygen isotope ratios.

5.2. The carbonate stable isotope record

Detrital carbonate clasts, probably derived from Carboniferous/Permian limestone, and limestone in the gravels of fluvial channel deposits have $\delta^{18}O$ and $\delta^{13}C$ values ranging from −19.0 to −8.5‰, and −7.5 to +10‰ respectively, generally overlapping with many of the $\delta^{18}O$

Table 1
Oxygen and carbon isotope data for microdrilled samples of different morphologies in the Linxia basin. Also see Fig. 9

Sample name	Subsample ID	Stratigraphic level (m)	Description (of carbonate or matrix hosting disseminated carbonate)	$\delta^{13}C$ (PDB)‰	$\delta^{18}O$ (PDB)‰
Maogou section					
MG362	a	129	Shell fragment	−6.23	−9.76
MG362	b		Micritic marl	−6.63	−10.60
MG362	c		Detrital clay-rich clast	−7.75	−9.81
MG362	d		Micritic marl	−6.26	−9.96
MG362	e		Micritic marl	−6.20	−10.05
CHOO10	1	152	Secondary void filling carbonate	−5.90	−9.76
CHOO10	5		Detrital carbonate clast	−5.82	−9.41
CHOO10	7		Siltstone	−5.61	−9.21
CHOO10	8		Detrital clay-rich clast	−5.74	−9.14
MG329	1	96	Detrital clay-rich clast	−6.06	−9.20
MG329	2		Secondary carbonate vein	−6.41	−9.63
MG329	3		Secondary clay-filled vein	−6.25	−9.40
MG329	4		Detrital clay-rich clast	−6.11	−9.14
MG329	5		Detrital clay-rich clast	−6.20	−9.46
MG329	6		Micritic marl	−5.92	−9.31
CHOO1′	1	136	Carbonate inter-clast cement	−6.27	−9.39
CHOO1′	3		Limestone clast in gravel	−6.17	−10.02
CHOO2	1	137	Micritic marl	−6.45	−9.75
CHOO2	3		Detrital carbonate clast	−6.02	−8.97
CHOO2	4		Detrital clay-rich clast	−5.79	−9.14
CHOO14	1	? (Upper Dongxiang)	Siltstone	−5.10	−8.13
CHOO14	2		Siltstone	−5.23	−8.38
CHOO14	3		Siltstone	−4.90	−8.01
CHOO14	4		Siltstone	−5.34	−8.49
CHOO14	6		Siltstone	−5.42	−8.97
CHOO14	7		Detrital clay-rich clast	−4.89	−7.53
Wangjiashan section					
CHOO31	1	230	Detrital carbonate clast	−2.87	−4.60
CHOO31	2		Micritic marl	−2.70	−3.88
CHOO31	3		Secondary clay-filled vein	−2.71	−4.24
CHOO32	1	254 or 250	Detrital carbonate clast	−3.11	−6.75
CHOO32	2		Detrital clay-rich clast	−3.47	−6.96
CHOO32	3		Micritic marl	−3.26	−7.79
CHOO34	1	424	Detrital carbonate clast	−8.65	−13.68
CHOO34	2		Secondary carbonate vein	−6.64	−9.46
CHOO34	3		Siltstone	−6.27	−8.89
CHOO36	1	474	Limestone clast in gravel	−7.04	−11.49
CHOO36	2		Carbonate inter-clast cement	−6.12	−9.78
CHOO36	2 (Repeat)		Carbonate inter-clast cement	−2.88	−10.19
CHOO36	3		Secondary carbonate vein	−6.19	−10.21
CHOO36	4		Secondary carbonate vein	−5.83	−9.59
CHOO36	5		Carbonate inter-clast cement	−0.58	−9.22
CHOO36	C1		Carbonate inter-clast cement	−1.18	−8.67
CHOO36	C2		Carbonate inter-clast cement	−0.84	−9.57
CHOO36	F		Carbonate inter-clast cement	−3.14	−10.67
CHOO36	G		Carbonate inter-clast cement	−1.80	−9.00
CHOO36	2.3		Limestone clast in gravel	0.21	−15.69
CHOO36	2.4		Limestone clast in gravel	−2.31	−10.27
CHOO36	2.5		Limestone clast in gravel	−3.74	−9.97
01WN43	A	278	Detrital carbonate clast	−5.01	−7.61
01WN43	B		Siltstone	−4.72	−7.38
01WN37	A	110	Siltstone (light grey)	−7.15	−12.04
01WN37	B		Siltstone (dark grey)	−8.00	−10.65

(continued on next page)

Table 1 (*continued*)

Sample name	Subsample ID	Stratigraphic level (m)	Description (of carbonate or matrix hosting disseminated carbonate)	$\delta^{13}C$ (PDB)‰	$\delta^{18}O$ (PDB)‰
Others					
CHOO35	0		Carboniferous/Permian Limestone	7.39	−9.92
CHOO35	2		Carboniferous/Permian Limestone	−7.38	−18.61
CHOO35	3		Carboniferous/Permian Limestone	−0.02	−14.54
CHOO06	1		Modern soil carbonate at 3.4 km	−7.06	−10.77
CHOO06	2		Modern soil carbonate at 3.4 km	−5.29	−11.21
CHOO06	4		Modern soil carbonate at 3.4 km	−4.88	−10.37
CHOO06	5		Modern soil carbonate at 3.4 km	−3.52	−9.49
CHOO06	6		Marble clast at 3.4 km	9.79	−8.57

values of authigenic carbonates in Linxia, but in many cases the isotopic values are different than the cementing carbonates around these clasts or in nearby micrites (Table 1, Fig. 9). The clearest example is the metamorphosed limestone gravels collected from conglomerates, such as CHOO-36 and CHOO-06.6. The very positive $\delta^{13}C$ and very negative $\delta^{18}O$ values of some of these gravels relative to authigenic carbonates indicate that most of the detrital limestones have significantly different isotopic compositions than authigenic carbonates they are intimately associated with (Table 1, Fig. 9). Because care was taken to avoid autochthonous limestone or dolomite in sampling we have minimized the influence of detrital carbonates in Fig. 5.

The variation in $\delta^{18}O$ values of the lake carbonates cannot be attributed solely to temperature. The calcite fractionation relationship with temperature is such that a change of ~4.3 °C leads to only a 1‰ change in the $\delta^{18}O$ value of calcite (Kim and O'Neil, 1997). Thus, a change of more than 30 °C would be required to account for the 7‰ variations of the lake carbonate $\delta^{18}O$ values in the Maogou section, which is very unlikely. The high frequency $\delta^{18}O$ variation also argues against major changes in the altitude of surrounding regions or continentality as a driver of $\delta^{18}O$ variability, because these factors, tied to tectonic processes, would not cause short-term change and rapid excursions.

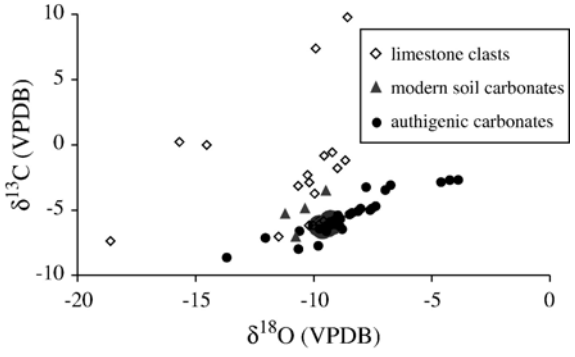

Fig. 9. Stable isotopic composition of carbonates in Table 1. Limestone clasts are of Carboniferous/Permian age. Modern soil carbonate formed under granite clasts in a soil zone at 3.4 km elevation on the northeastern edge of the Tibetan Plateau. Authigenic carbonates include shell fragments, carbonate cements, marl and micritic carbonate.

Therefore, the relationship between $\delta^{18}O$ values and carbonate mineralogy in the Linxia basin leads to the idea that more negative $\delta^{18}O$ values represent open-lake conditions, and more positive $\delta^{18}O$ values represent closed and evaporative lake conditions. This conclusion is supported by the linear and positive correlation between the $\delta^{18}O$ and $\delta^{13}C$ values in the lacustrine facies (Fig. 10). This covariation is expected for a lake switching between open and closed states (Talbot, 1990; Drummond et al., 1995). During open basin conditions, the $\delta^{18}O$ value of lake water approaches the value of inflowing water, which is usually derived from the rainfall in the basin catchments, perhaps biased toward higher elevations around the basin. Although there is a good deal of variability in the record, $\delta^{18}O$ values of both marls and cements maintain a value of approximately −9‰ as the most negative end member between 13.1 and 5.3 Ma in the Maogou section. This −9‰ value is perhaps tied to the $\delta^{18}O$ of meteoric water in the Linxia basin. Fresh water input often leads to lower pH conditions in the lake, reducing the alkalinity of the lake, which can lead to more negative $\delta^{13}C$ values due to vigorous atmospheric exchange or the input of DIC with much more negative $\delta^{13}C$ values derived from soil carbon oxidation (Li and Ku, 1997). Under closed basin conditions, high evaporation increases alkalinity and the $\delta^{18}O$ values of lake water increase. Higher $\delta^{13}C$ values could be the result of high productivity due to high nutrient concentration, or outgassing of CO_2 (Talbot, 1990). A weak covariation is also found in the Linxia basin fluvial facies (Fig. 10) that could also

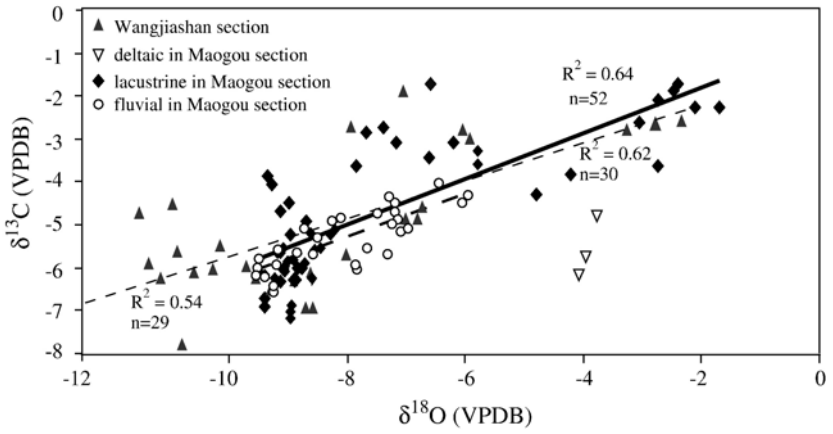

Fig. 10. Stable isotopic composition of all authigenic carbonates deposited in the Linxia basin between 13.1 and 4.3 Ma. Note the covariation between $\delta^{18}O$ and $\delta^{13}C$ values.

be created by evaporation of the groundwaters of the region.

5.3. C/N ratio, % C, $\delta^{13}C_{org}$ and selective organic matter degradation

The C/N ratio of organic matter in sediments is generally used as an indicator of the source of the organic matter and of the degree of modification from its original state (Meyers and Benson, 1988). Because terrestrial plants are protein-poor and cellulose-rich, the C/N ratio of terrestrial plants is higher than aquatic algae, with C_3 plants typically >15 and C_4 plants >35. Fresh-water algae are protein-rich and cellulose-poor, and have C/N ratios between 4 and 10 (Meyers, 1994, 2003). C/N ratios in most of the fine sediments of the Linxia basin are low (Fig. 5), which is usually interpreted as an indicator that the organic material is derived from aquatic primary production. However, in this record there are numerous intervals where the C/N ratio is significantly less than 4, a value that is too low for aquatic algae. Selective degradation of the organic matter during diagenesis can modify the original C/N ratio of organic matter (Meyers and Ishiwatari, 1993; Meyers, 1994; Sampei and Matsumoto, 2001). The C/N ratio of organic matter can decrease during diagenesis (Muller, 1977; Meyers and Ishiwatari, 1993; Meyers, 1997; Lehmann et al., 2002), with loss of organic matter followed by the fixing of inorganic nitrogen as ammonium or nitrate compounds on clays or mineral surfaces, especially when the final organic content of the sediment is very low (Muller, 1977; Thornton and McManus, 1994; Muller and Mathesius, 1999; Sampei and Matsumoto, 2001). The loss of initial organic matter can be very fast in nature (Eadie et al., 1984; Melillo et al., 1989; Freudenthal et al., 2001), and Muller (1977) shows an example of early diagenesis of oxidized pelagic sediments shifting C/N ratios to <4 in intervals where the % C is <0.3. Thus, the very low % C in the Linxia basin and the anomalously low C/N ratios suggest that the organic matter in the Linxia basin has experienced significant losses through diagenetic degradation. If this is the case, the value of 10 usually used to differentiate lake algae and terrestrial organics may not apply to these very old sediments and we cannot interpret the C/N ratio as simple indicator of the source (terrestrial vs. aquatic) of organic matter in the Linxia basin.

In general, the carbon isotope ratio of organic matter, $\delta^{13}C_{org}$, of lake sediments is controlled by algae production and the proportion of C_3 and C_4 land plants in the lake's catchment (Meyers, 1994, 2003). Modern terrestrial plants using the C_3 pathway have an average $\delta^{13}C_{org}$ value of about −27.5‰ VPDB and those using the C_4 pathway are around −13‰ (Farquhar et al., 1989). The $\delta^{13}C_{org}$ of the typical lake algae in fresh water is about −28‰ (Meyers, 1994, 2003). When discussing samples collected in pre-industrial times, these three $\delta^{13}C$ values should be increased by 1 to 1.5‰ to account for fossil fuel burning (Farquhar et al., 1989). The $\delta^{13}C_{org}$ value has been seen to increase as high as −9‰ when lake waters are carbon-limited and productivity is unusually high, and it can decrease to −32‰ when large amounts of DIC derived from soil systems are added to the lake (Meyers, 1994, 2003). The $\delta^{13}C_{org}$ values in the Linxia basin are within this range of $\delta^{13}C$ values characterized of both lacustrine algae and C_3 land plants (Meyers, 1997, 2003) (Fig. 5).

Alteration and degradation of organic matter in sediments may lead to a change in its carbon isotope

ratio, but other studies have shown that this shift is relatively small; in almost all cases less than 2‰. Early diagenetic degradation of organic matter seems to result in a 0‰ to 4‰ decrease in the $\delta^{13}C_{org}$ values through the preferential removal of ^{13}C-enriched compounds (Spiker and Hatcher, 1984; Prahl et al., 1997; Freudenthal et al., 2001). Small changes in the carbon isotopic composition of the soil organic matter were also observed during litter decay (Melillo et al., 1989). In lacustrine settings, a recent study from Lake Lugano suggests that the eutrophic sediments are depleted by about 1.5‰ in ^{13}C with respect to sinking organic matter, which is in agreement with a 1.6‰ decrease in the $\delta^{13}C_{org}$ value seen within three months during an incubation-based diagenesis experiment (Lehmann et al., 2002). However, studies of long-term diagenesis of organics in sediments suggest that the $\delta^{13}C_{org}$ values of highly altered organic matter may be up to 2‰ more positive than the original $\delta^{13}C$ value (Hatté et al., 1999; Krull and Skjemstad, 2003; Liu et al., 2003). The % C of a highly weathered soil (oxisol) in Australia decreases from 8.19 % at the surface to 0.57 % at 120–140 cm depth in the soil profile, and $\delta^{13}C_{org}$ values change from −26‰ to −24.5‰. It has been suggested that the ^{13}C-enrichment in the oxisol was caused by selective preservation of plant compounds more enriched in ^{13}C (physical protection of C through microaggregation with soil oxides and clays) (Krull and Skjemstad, 2003). The % C and C/N ratios of loess sequences in the eastern Chinese Loess Plateau and in Nuβloch, Germany average 0.3 % and 2 to 4 respectively (Hatté et al., 1999; Liu et al., 2003), showing that loess is very similar to the Linxia basin sediments in organic preservation. Carbon isotope ratios of these loess sections remain in the −25.5 to −22.0‰ range, reflecting their location in regions dominated by C_3 plants. The $\delta^{13}C_{org}$ values of Nuβloch loess shift from −25.5‰ to an average of −24.2‰ down section, and the authors suggest these values result from the degradation of a vegetation assemblage with a strong predominance of C_3 plants (Hatté et al., 1999). Therefore, we conclude that, although the Linxia basin sediments have seen strong degradation of organic matter, this results in only a small shift in the $\delta^{13}C_{org}$ values.

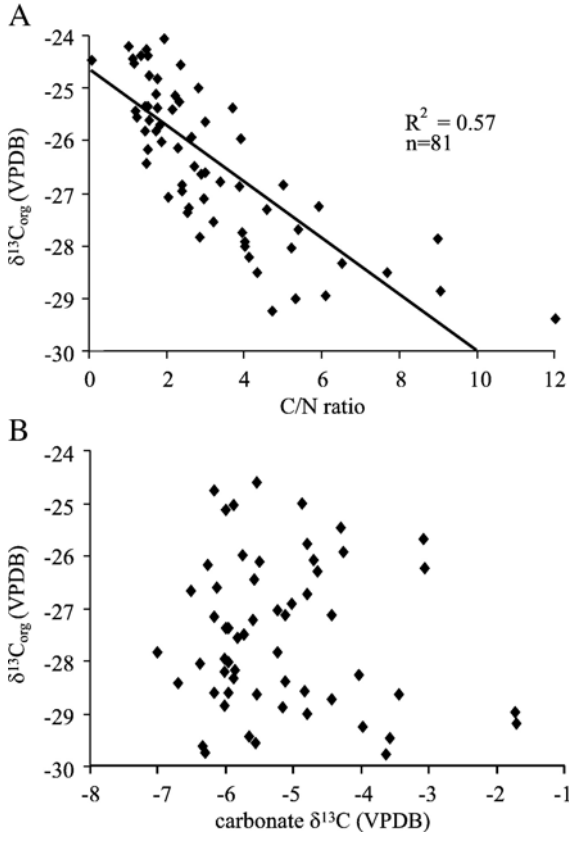

Fig. 11. (A) C/N and $\delta^{13}C_{org}$ are negatively correlated in the Linxia basin. (B) $\delta^{13}C_{org}$ vs. $\delta^{13}C_{carbonate}$ in the Linxia basin.

5.4. Environmental significance of $\delta^{13}C_{org}$ in the Linxia basin

A negative correlation between $\delta^{13}C_{org}$ and C/N values exists in the Linxia basin, with the highest C/N ratio associated with lowest $\delta^{13}C_{org}$ values (Fig. 11A). The negative correlation could be explained by variation in the balance between internal lake productivity and terrestrial organic matter input. If variation in algal productivity is the dominant control on $\delta^{13}C_{org}$ values, then one would expect a correlation between $\delta^{13}C_{org}$ and $\delta^{13}C$ of carbonate as they both are derived from the same lake water, and higher productivity should lead to more positive $\delta^{13}C$ values for both organics and carbonates. There is no correlation between $\delta^{13}C_{org}$ and carbonate $\delta^{13}C$ values (Fig. 11B) in the Linxia basin, which suggests that terrestrial plant matter contributes significantly to the organic matter in the sediment. A pollen study from the same section also indicates that significant amounts of terrestrial plant pollen have been preserved in the lake sediments (Ma et al., 1998). The negative correlation of C/N ratio and $\delta^{13}C_{org}$ suggests that, despite a general lowering of C/N ratios due to loss of organic matter and/or the retention of inorganic N, the higher C/N ratios displayed by terrestrial plants are associated with the most negative $\delta^{13}C_{org}$ values. This suggests that these terrestrial plants probably used the C_3 photosynthetic pathway. The relatively stable and very negative $\delta^{13}C_{org}$ values (−24

to −29‰) throughout the record, with the highest C/N ratio associated with the most negative values, suggest that terrestrial C_4 grasses were either absent or insignificant in the Linxia region prior to 4.3 Ma, although C_4 grasses are significant in the region at present (Yin and Li, 1997; Wang and Deng, 2005). This is in agreement with a $\delta^{13}C$ record of mammalian tooth enamel from the Linxia basin, which indicates that there were no significant C_4 plants in the Linxia basin before 2–3 Ma (Wang and Deng, 2005). This observation also agrees with other studies that conclude that C_4 plant expansion in the north of the Tibetan Plateau occurred later than the expansion in the south (Quade et al., 1989; Ding and Yang, 2000; Sanyal et al., 2004).

5.5. Lake hydrology and climate history of the Linxia basin between 13.1 and 4.3 Ma

Before ~8.0 Ma, the Linxia basin was in a relatively stable tectonic setting, a foredeep depozone (Fang et al., 2003). Due to the continuous flexural loading of the NE edge of the Tibetan Plateau and the thick foredeep sediments, it seems highly unlikely that the frequent oscillations between closed and open lake conditions in the Linxia basin (13.1 to 8.0 Ma) were tectonically driven. Climate variability is a much more likely cause of the frequent changes in lake hydrology and for the relationship between $\delta^{18}O$ values and carbonate mineralogy (Fig. 7). More negative $\delta^{18}O$ values occur when the climate is cool and lake open, resulting in short water residence time in the lake and little evaporation. Conversely, high $\delta^{18}O$ and $\delta^{13}C$ values indicate lake closure and low lake levels, which result in strong evaporation and elevated salinity. Note that this variation occurs on both the meter scale level, between different carbonate layers, and on the millimeter scale, as shown in sample MG252 (Fig. 8).

Based on the stable isotope records shown in Figs. 5 and 6, we can summarize the climatic and hydrological conditions in the Linxia basin between 13.1 and 4.3 Ma as follows. Climate varied frequently between dry and wet during the times of strong $\delta^{18}O$ variation, and the lake experienced frequent shifts between closed and open conditions between 13.1 and 8.0 Ma. Dolomite formed when lake levels were low, the lake was closed and more saline, and $\delta^{18}O$ values were high; these were times of more arid conditions. There is a period of enhanced dryness between 9.6 Ma and 8.5 Ma, during which (a). the frequency of marls in lake sediments increases dramatically, (b). the $\delta^{18}O$ values of the carbonates reach maximum values, and (c). shallow water sediments increase due to a drop in lake level (Fan et al., 2006). This arid event seems to be contemporaneous with the 3‰ shift to more positive $\delta^{18}O$ values in soil carbonates in Pakistan (Quade et al., 1989), which occurred beginning at ~9.5 Ma (after conversion of that paper's magnetochronology to that of Cande and Kent, 1995). This shift is interpreted as a regional climate change preceding a change from C_3 to C_4 plant dominated landscapes in Pakistan (Quade et al., 1989). The pollen record from the Maogou section in the Linxia basin shows an increase to 50% grasses and a sharp decrease in conifers beginning at about 9.2 Ma (Ma et al., 1998; Li and Fang, 1999 — note that the chronology used in this paper matches that in Li and Fang, 1999).

After 8.0 Ma, the regional climate became more humid and the lake basin opened, as is shown by less frequent marls and stable, low $\delta^{18}O$ values. At 6.2 Ma, the basin was entrained in the uplift at the edge of the Tibetan Plateau, and the depositional setting at the basin center switched from lacustrine to fluvial. However, the $\delta^{18}O$ values of the fluvial carbonates are unchanged at this time, consistent with the idea that the basin drainage system was open and the $\delta^{18}O$ values of waters were controlled primarily by the isotopic composition of rainfall and runoff. In this case the filling of the lake basin and switch to fluvial conditions would not change the oxygen isotope ratio of surface waters. This also suggests that the deformation in the northeastern Tibetan Plateau around 6.2 Ma was not accompanied by major changes in water sources or the isotopic composition of the atmospheric vapor at this time. Our interpretation of the isotope record disagrees with the pollen record, which is dominated by grasses in the 8.0 to 6.7 Ma interval — pollen shows a return to wetter conditions beginning at 6.7 until 5.5 Ma (Li and Fang, 1999).

After 5.3 Ma, either increased aridity or cooler temperatures (or both) led to a gradual increase in $\delta^{18}O$ values. Although it is impossible to separate the two factors (cooler or dryer) in the stable isotope record, there is corollary evidence for both processes at this time. Aridity could increase the $\delta^{13}C_{org}$ values by affecting the water use efficiency of terrestrial C_3 plants (Ehleringer, 1988), and increase the $\delta^{18}O$ and $\delta^{13}C$ values of carbonates by strong evaporation. Cooler climate could also increase the $\delta^{18}O$ and $\delta^{13}C$ values of carbonates by larger fractionation between water and carbonates. Pollen in the Maogou section becomes nearly 100% grass at 5.3 Ma and grasses dominate to the end of this record at 4.3 Ma (Li and Fang, 1999). Grain-size records of eolian sediments in the Linxia basin point to a major intensification of the Asian winter monsoon at 5.3 Ma (Fan et al., 2006), which would lead to a colder and dryer climate.

We should point out, however, that other studies have suggested more humid Pliocene conditions farther east on the central Loess Plateau due to an increase in East Asian summer monsoon rainfall (Ding et al., 1999). These studies may not be contradictory as the impact of a strengthened summer or winter monsoon on the average annual climate may differ along the gradient in aridity from east to west. Regional cooling at this time is consistent with global trends: deep-sea temperature and sea levels drop at ~5.5 Ma (Lear et al., 2000; Billups and Schrag, 2002).

6. Conclusions

This multi-proxy study has documented a long-term climate and environmental change in the Late Miocene and Early Pliocene at the northeastern corner of the Tibetan Plateau from 13.1 to 4.3 Ma. Carbonate petrology and the stable isotope ratios of different carbonate forms show that carbonates in the Linxia basin have experienced some degree of diagenesis. However, oxygen isotope variability on both the millimeter and meter scale suggests that diagenesis is early, geologically contemporaneous with carbonate formation. Therefore, $\delta^{18}O$ values still carry the geochemical signature of original surface conditions. In the case of lacustrine micrites, isotope ratios reflect lake water conditions, with frequent oscillations between more negative LMC $\delta^{18}O$ values and more positive dolomite $\delta^{18}O$ values arising from changing degrees of lake closure and evaporation.

The organic matter preserved in the Linxia basin is a mixture of terrestrial plant matter and lake algae. The lack of correlation between $\delta^{13}C_{org}$ and carbonate $\delta^{13}C$ values in the Linxia basin suggests that terrestrial plant matter makes a significant contribution. The organic matter content in the sediments of the Maogou section is very low, typically less than 0.2%. This has led to the retention of inorganic nitrogen in the sediments as organic carbon is lost to diagenesis, which in turn lowers the C/N ratio of remaining organics. The typical range of C/N ratios used to distinguish terrestrial and aquatic organics may therefore not apply in the Linxia basin. Degradation is unlikely to have changed the $\delta^{13}C_{org}$ values of the organic matter in the Linxia basin. Relatively invariant and low $\delta^{13}C_{org}$ values throughout the section are in agreement with previous studies that concluded that C_4 grasses were either absent or insignificant in the Linxia region prior to 4.3 Ma.

Hydrological variation of the Linxia basin is mostly controlled by regional climate. From 13.1 to 8.0 Ma, the basin varied frequently between open and closed conditions suggesting climate cycling between arid and humid conditions. Aridity reached its maximum at 9.6–8.5 Ma. From 8.0 to 5.3 Ma, a stable humid climate dominated the region. After 5.3 Ma, the climate became gradually drier and/or cooler.

Acknowledgements

We would like to thank Jay Quade and Andy S. Cohen for valuable discussions. The paper has benefited from careful reviews by two anonymous reviewers. C.S and X.F are thankful to Chinese National Science Foundation Grants 90211013 and 40421101, and Chinese National Key Project on Basic Research (grant 2005CB422001).

References

An, Z., Kutzbach, J.E., Prell, W.L., Porter, S.C., 2001. Evolution of Asian monsoons and phased uplift of the Himalaya–Tibetan plateau since Late Miocene times. Nature 411, 62–66.

Billups, K., Schrag, D.P., 2002. Paleotemperatures and ice volume of the past 27 Myr revisited with paired Mg/Ca and $^{18}O/^{16}O$ measurements on benthic foraminifera. Paleoceanography 17 (1), 26–37.

Cande, S.C., Kent, D.V., 1995. Revised calibration of the geomagnetic polarity timescale for the late Cretaceous and Cenozoic. Journal of Geophysical Research 100 (B4), 6093–6095.

Dean, W.E., Stuiver, M., 1993. Stable carbon and oxygen isotope studies of the sediments of Elk Lake, Minnesota. In: Bradbury, J.P., Dean, W.E. (Eds.), Elk Lake, Minnesota: Evidence for Rapid Climate Change in the North-Central United States. Geological Society of America Special Paper, vol. 276, pp. 63–180.

Dettman, D.L., Fang, X., Garzione, C.N., Li, J., 2003. Uplift-driven climate change at 12 Ma: a long $\delta^{18}O$ record from the NE margin of the Tibetan plateau. Earth and Planetary Science Letters 214, 267–277.

Ding, Z.L., Yang, S.L., 2000. C_3/C_4 vegetation evolution over the last 7.0 Myr in the Chinese Loess Plateau: evidence from pedogenic carbonate $\delta^{13}C$. Palaeogeography, Palaeoclimatology, Palaeoecology 160, 291–299.

Ding, Z.L., Xiong, S.F., Sun, J.M., Yang, S.L., Gu, Z.Y., Liu, T.S., 1999. Pedostratigraphy and paleomagnetism of a 7.0 Ma eolian loess-red clay sequence at Lingtai, Loess Plateau, north-central China and the implications for paleomonsoon evolution. Palaeogeography, Palaeoclimatology, Palaeoecology 152, 49–66.

Ding, Z.L., Yang, S.L., Sun, J.M., Liu, T.S., 2001. Iron geochemistry of loess and red clay deposits in the Chinese Loess Plateau and implications for long-term Asian monsoon evolution in the last 7.0 Ma. Earth and Planetary Science Letters 185, 99–109.

Drummond, V.N., Patterson, W.P., Walker, J.C.G., 1995. Climate forcing of carbon-oxygen isotopic covariance in temperate region marl lakes. Geology 23, 1031–1034.

Eadie, B.J., Chambers, R.L., Gardner, W.S., Bell, G.L., 1984. Sediment trap studies in Lake Michigan: resuspension and chemical fluxes in the southern basin. Journal of Great Lakes Research 10, 307–321.

Ehleringer, J.R., 1988. Carbon isotope ratios and physiological processes in aridland plants. In: Rundel, P.W., Eheringer, J.R., Nagy, K.A. (Eds.), Applications of Stable Isotopic Ratios to Ecological Research. Springer-Verlag, New York, pp. 41–45.

Fan, M., Song, C., Dettman, D.L., Fang, X., Xu, X., 2006. The late Miocene and Pliocene atmospheric circulation recorded in the Linxia basin, Northeast Tibetan Plateau. Earth and Planetary Science Letters 248, 171–182.

Fang, X., Li, J., Wang, J., Zhong, W., Cao, J., 1995. Records of the uplift of the Qinghai–Xizang (Tibetan) Plateau and long-term climate change. In: Li, J. (Ed.), Uplift of Qinghai–Xizang (Tibet) Plateau and Global Change. Lanzhou University Press, Lanzhou, pp. 19–83.

Fang, X., Garzione, C.N., Van der Voo, R., Li, J., Fan, M., 2003. Flexural subsidence by 29 Ma on the NE edge of Tibet from the magnetostratigraphy of Linxia basin, China. Earth and Planetary Science Letters 210, 545–560.

Farquhar, G.D., Ehleringer, J.R., Hubrick, K.T., 1989. Carbon isotopic discrimination and photosynthesis. Annual Review of Plant Physiology and Plant Molecular Biology 40, 503–537.

Freudenthal, T., Wagner, T., Wenzhofer, F., Zabel, M., Wefer, G., 2001. Early diagenesis of organic matter from sediments of the eastern subtropical Atlantic: evidence from stable nitrogen and carbon isotopes. Geochimica et Cosmochimica Acta 65, 1795–1808.

Gansu Geologic Bureau, 1989. Regional Geologic History of Gansu Province. Geologic Publishing House, Beijing.

Garzione, C.N., Dettman, D.L., Horton, B.K., 2004. Carbonate oxygen isotope paleoalmetry: evaluating the effect of diagenesis on paleoelevation estimates for the Tibetan Plateau. Palaeogeography, Palaeoclimatology, Palaeoecology 212, 119–140.

Garzione, C.N., Ikari, M.J., Basu, A.R., 2005. Source of Oligocene to Pliocene sedimentary rocks in the Linxia Basin in northeastern Tibet from Nd isotopes: implications for tectonic forcing of climate. GSA Bulletin 117, 1156–1166.

Hatté, C., Antoine, P., Fontugne, M., Rousseau, D.D., Tisnérat-Laborde, N., Zöller, L., 1999. New chronology and organic matter $\delta^{13}C$ paleoclimatic significance of Nuβloch loess sequence (Rhine Valley, Germany). Quaternary International 62, 85–91.

Horton, B.K., Dupont-Nivet, G., Zhou, J., Waanders, G.L., Butler, R.F., Wang, J., 2004. Mesozoic–Cenozoic evolution of the Xining-Minhe and Dangchang basins, northeastern Tibetan Plateau: magnetostratigraphic and biostratigraphic results. Journal of Geophysical Research 109 (B04402). doi:10.1029/2003JB002913.

Kashiwaya, K., Shinaya, O., Hideo, S., Takayoshi, K., 2001. Orbit-related long-term climate cycles revealed in a 12-Myr continental record from Lake Baikal. Nature 410, 71–74.

Kim, S., O'Neil, J.R., 1997. Equilibrium and nonequilibrium oxygen isotope effects in synthetic carbonates. Geochimica et Cosmochimica Acta 61, 3461–3475.

Krull, E.S., Skjemstad, J.O., 2003. $\delta^{13}C$ and $\delta^{15}N$ profiles in ^{14}C-dated Oxisol and Vertisols as a function of soil chemistry and mineralogy. Geoderma 112, 1–29.

Last, W.M., 1990. Lacustrine dolomite; an overview of modern, Holocene, and Pleistocene occurrences. Earth-Science Reviews 27, 221–263.

Lear, C.H., Elderfield, H., Wilson, P.A., 2000. Cenozoic deep-sea temperatures and global ice volumes from Mg/Ca in benthic foraminiferal calcite. Science 287, 269–272.

Lehmann, M.F., Bernasconi, S.M., Barbieri, A., McKenzie, J.A., 2002. Preservation of organic matter and alteration of its carbon and nitrogen isotope composition during simulated and in situ early sedimentary diagenesis. Geochimica et Cosmochimica Acta 66, 3573–3584.

Li, H.C., Ku, T.L., 1997. $\delta^{13}C$–$\delta^{18}O$ covariance as a Paleohydrological indicator for closed-basin lakes. Palaeogeography, Palaeoclimatology, Palaeoecology 133, 69–80.

Li, J., Fang, X., 1999. Uplift of the Tibetan Plateau and environmental changes. Chinese Science Bulletin 44, 2117–2124.

Liu, W., An, Z., Zhou, W., Head, M.J., Cai, D., 2003. Carbon isotope and C/N ratios of suspended matter in rivers; an indicator of seasonal change in C_4/C_3 vegetation. Applied Geochemistry 18, 1241–1249.

Ma, Y., Li, J., Fang, X., 1998. A record of polynoflora and climatic evolution of Red Bed between 30.6 to 5.0 MaBP, Linxia Basin. Chinese Science Bulletin 43, 301–304 (in Chinese).

Métivier, F., Gaudemer, Y., Tapponnier, P., Meyer, B., 1998. Northeastward growth of the Tibet plateau deduced from balanced reconstruction of two depositional areas: the Qaidam and Hexi Corrodor basins, China. Tectonics 17, 823–842.

Meyers, P.A., 1994. Preservation of elemental and isotopic source identification of sedimentary organic matter. Chemical Geology 114, 289–302.

Meyers, P.A., 1997. Organic geochemical proxies of paleoceanographic, paleolimnologic, and paleoclimatic processes. Organic Geochemistry 27, 213–250.

Meyers, P.A., 2003. Applications of organic geochemistry to paleolimnological reconstructions: a summary of examples from the Laurentian Great Lakes. Organic Geochemistry 34, 261–289.

Meyers, P.A., Benson, L.V., 1988. Sedimentary biomarker and isotopic indicators of the paleoclimatic history of the Walker Lake basin, western Nevada. Organic Geochemistry 13, 807–813.

Meyers, P.A., Ishiwatari, R., 1993. Lacustrine organic geochemistry—an overview of indicators of organic matter sources and diagenesis in lake sediments. Organic Geochemistry 20, 867–900.

Melillo, J.M., Aber, J.D., Linkins, A.E., Ricca, A., Fry, B., Nadelhoffer, K.J., 1989. Carbon and nitrogen dynamics along the decay continuum: plant litter to soil organic matter. Plant and Soil 115, 189–198.

Muller, P.J., 1977. C/N ratios in Pacific deep-sea sediments: effect of inorganic ammonium and organic nitrogen compounds sorbed by clays. Geochimica et Cosmochimica Acta 41, 765–776.

Muller, A., Mathesius, U., 1999. The palaeoenvironments of coastal lagoons in the southern Baltic Sea, I. The application of sedimentary C/N ratios as source. Palaeogeography, Palaeoclimatology, Palaeocology 145, 1–16.

Prahl, F.G., de Lange, G.J., Scholten, S., Cowie, G.L., 1997. A case of post-depositional aerobic degradation of terrestrial organic matter in turbidite deposits from the Madeira Abyssal Plain. Organic Geochemistry 27, 141–152.

Quade, J., Cerling, T.E., Bowman, J.R., 1989. Development of Asian monsoon revealed by marked ecological shift during the latest Miocene in northern Pakistan. Nature 342, 163–166.

Rea, D.K., Snoeckx, H., Joseph, L.H., 1998. Late Cenozoic eolian deposition in the North Pacific: Asian drying, Tibetan uplift, and cooling of the northern hemisphere. Paleoceanography 13 (3), 215–224.

Sampei, Y., Matsumoto, E., 2001. C/N ratios in a sediment core form Nakaumi Lagoon, southwest Japan — usefulness as an organic source indicator. Geochemical Journal (Japan) 35, 189–205.

Sanyal, P., Bhattacharya, S.K., Kumar, R., Ghosh, S.K., Sangode, S.J., 2004. Mio-Pliocene monsoonal record from Himalayan foreland basin (Indian Siwalik) and its relation to vegetational change. Palaeogeography, Palaeoclimatology, Palaeocology 205, 23–41.

Schmidt, M., Xeflide, S., Botz, R., Mann, S., 2005. Oxygen isotope fractionation during synthesis of CaMg-carbonate and implications for sedimentary dolomite formation. Geochimica et Cosmochimica Acta 69, 4665–4674.

Spiker, E.C., Hatcher, P.G., 1984. Carbon isotope fractionation of sapropelic organic matter during early diagenesis. Organic Geochemistry 5, 283–290.

Sun, J., 2002. Provenance of loess material and formation of loess deposits on the Chinese Loess Plateau. Earth and Planetary Science Letters 203, 845–859.

Talbot, M.R., 1990. A review of the palaeohydrological interpretation of carbon and oxygen ratios in primary lacustrine carbonates. Chemical Geology 80, 261–279.

Thornton, S.F., McManus, J., 1994. Application of organic carbon and nitrogen stable isotope and C/N ratios as source indicators of organic matter provenance in estuarine systems: evidence from the Tay Estuary, Scotland. Estuarine, Coastal and Shelf Science 38, 219–233.

Vasconcelos, C., McKenzie, J.A., Warthmann, R., Bernasconi, S.M., 2005. Calibration of the $\delta^{18}O$ paleothermometer for dolomite precipitated in microbial cultures and natural environments. Geology 33, 317–320.

Warren, J., 2000. Dolomite: occurrence, evolution and economically important associations. Earth-Science Reviews 52, 1–81.

Wang, Y., Deng, T., 2005. A 25 m.y. isotopic record of paleodiet and environmental change from fossil mammals and paleosols from the NE margin of the Tibetan Plateau. Earth and Planetary Science Letters 236, 332–338.

Yin, L., Li, M., 1997. A study of the geographic distribution and ecology of C4 plants in China: I. C4 plant distribution in China and their relation with regional climatic condition. Acta Ecologica Sinica 17, 350–363.

Zachos, J., Pagani, M., Sloan, L., Thomas, E., Billup, K., 2001. Trends, rhythms, and aberrations in global climate 65 Ma to present. Science 292, 686–693.

Zheng, H., Powell, C.M., Rea, D.K., Wang, J., Wang, P., 2004. Late Miocene and mid-Pliocene enhancement of the East Asian monsoon as viewed from the land and sea. Global and Planetary Change 41, 147–155.